Title: Wired for function: Anatomical connectivity patterns predict face-selectivity in the fusiform gyrus

Authors: Zeynep M. Saygin[*], David E. Osher[*], Kami Koldewyn, Gretchen Reynolds, John D.E. Gabrieli, Rebecca R. Saxe

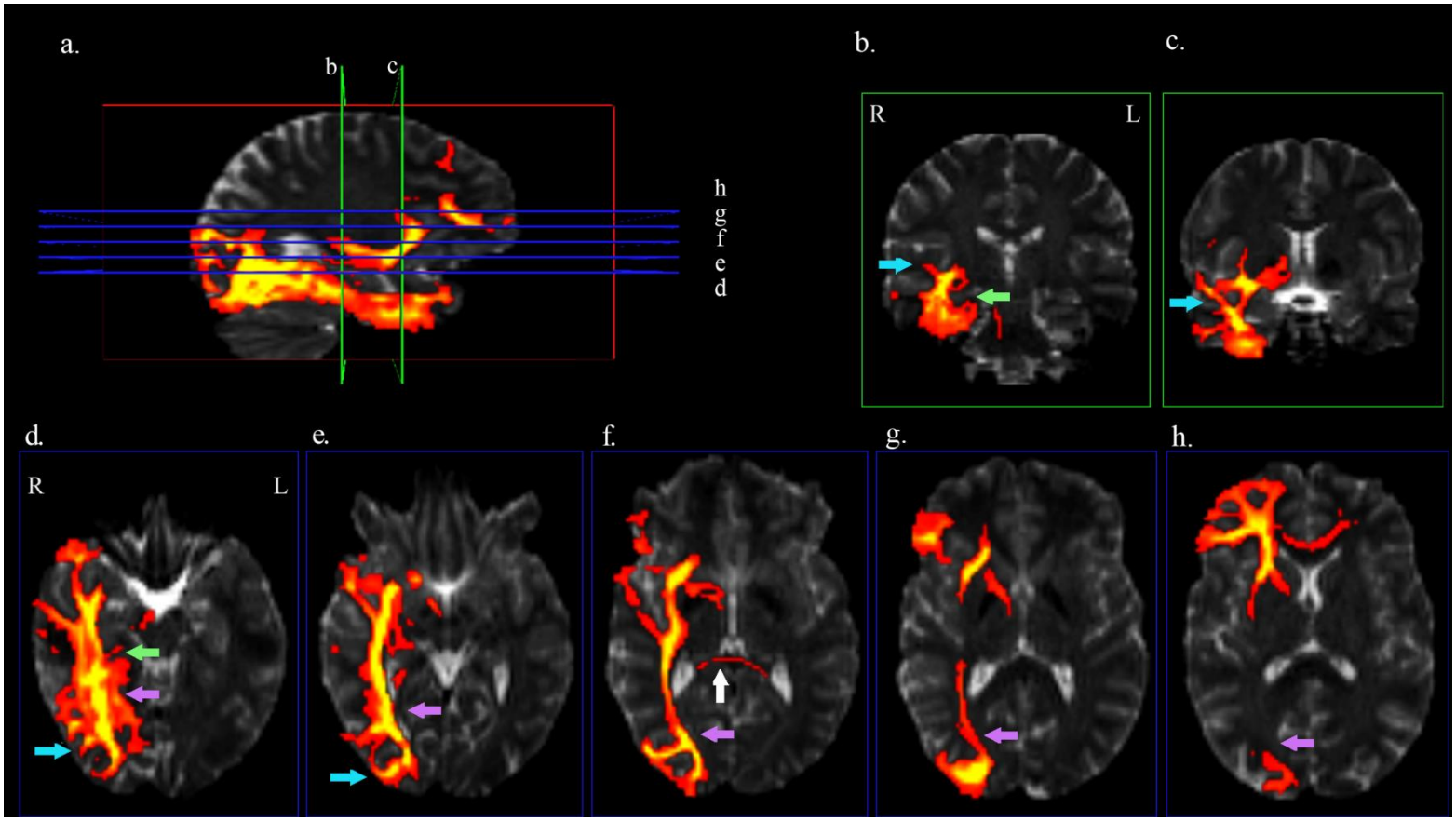

Supplementary Figure 1. Probabilistic tracts for an example subject, overlaid on the same subject's low-b diffusion images. These depict all possible tracts that the tractography algorithm used to connect the fusiform directly or indirectly with other brain regions. These tracts are naïve to functional selectivity in the fusiform. **a.** Right sagittal section showing the inferior longitudinal fasiculus (ILF), which travels inferiorly to the unicinate, as well as the superior longitudinal fasiculus (SLF), and short/U-fibers. It also displays the slice locations for coronal slices (green boxes; **b** and **c**) and axial slices (blue boxes; **d** through **h**). The fibers of the inferior longitudinal fasiculus (ILF; purple arrows in **d** through **h**) run anteriorly, connecting the lateral occipital cortex, lingual and fusiform gyri. The ILF then projects laterally to superior, middle, and inferior temporal gyri, and medially to the parahippocampal gyrus (green arrows in **b** and **d**). The forceps major connects the left and right medial cortices (white arrow in **f**) while the U-shaped fibers (blue arrows in coronal sections **b** and **c**; axial sections **d** and **e**) are lateral to the ILF and connect adjacent gyri of the lateral occipito-temporal cortex.

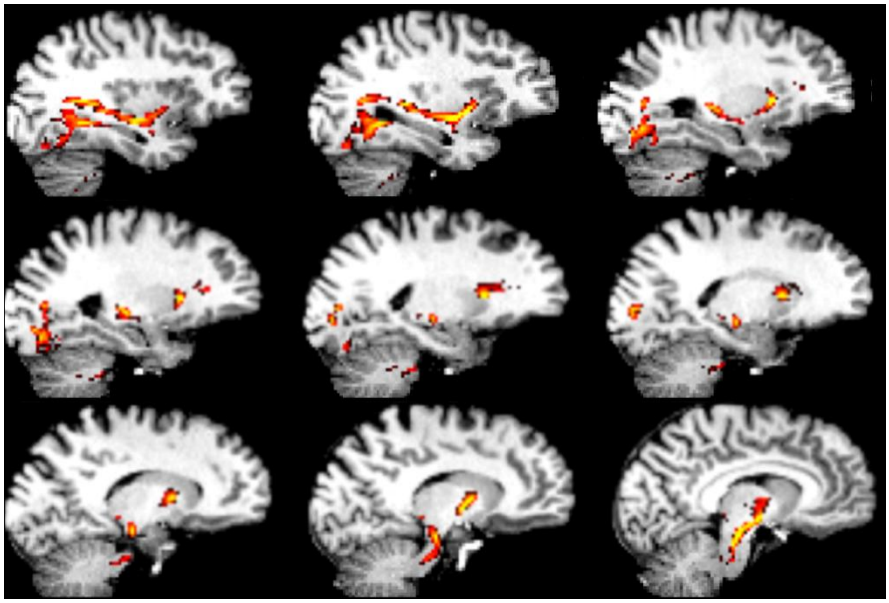

Supplementary Figure 2. Probabilistic tracts overlaid on the subject's anatomical image that was registered to the diffusion images. The sagittal sections on the right hemisphere show possible multisynaptic pathways that the probabilistic algorithm takes from extrastriate cortex, through the pons, and to the cerebellar pathways.

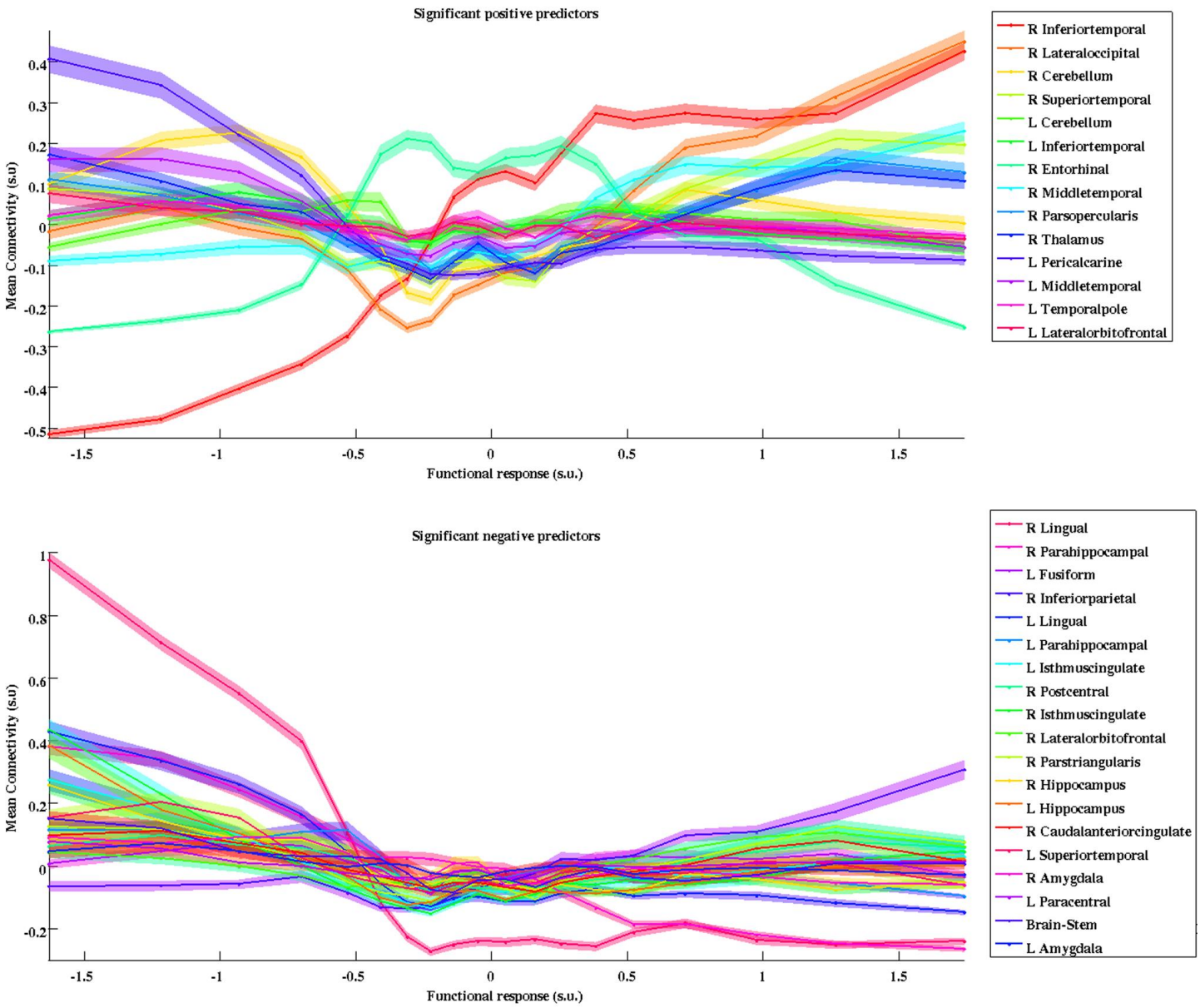

Supplementary Figure 3. Relationship between connectivity and selectivity. Mean connectivity weights for the significantly predictive targets (**a** positive, **b** negative) are plotted for groups of voxels binned by their functional selectivity, sliding across each fifth percentile. Shaded regions represent standard error.

Supplementary Table 1. Face-selective fusiform voxels have different connectivity patterns than scene-selective voxels. Thirty-four out of eighty-five targets were significantly different across subjects, Bonferonni corrected at $P < 0.05/85$.

Target	p	F
R Inferiortemporal	ε	1194.29
R Lingual	ε	633.70
R Parahippocampal	ε	231.07
R Middletemporal	ε	146.25
R Cerebellum	ε	111.97
R Isthmuscingulate	ε	99.37
R Lateraloccipital	1.22×10^{-15}	65.56
L Inferiortemporal	3.00×10^{-15}	63.64
L Isthmuscingulate	6.41×10^{-13}	52.66
R Hippocampus	9.50×10^{-13}	51.85
R Superiortemporal	1.46×10^{-12}	50.98
R Amygdala	4.44×10^{-12}	48.73
R Precuneus	8.50×10^{-11}	42.76
L Cerebellum	1.25×10^{-10}	41.99
L Hippocampus	2.89×10^{-09}	35.69
L Pericalcarine	1.71×10^{-08}	32.15
L Precuneus	3.52×10^{-08}	30.72
L Cuneus	7.95×10^{-08}	29.11
R Pallidum	1.11×10^{-07}	28.45
R Thalamus	1.69×10^{-07}	27.62
R Cuneus	7.80×10^{-07}	24.62
R Supramarginal	9.95×10^{-07}	24.14
R Parsorbitalis	3.82×10^{-06}	21.52
R Pericalcarine	6.80×10^{-06}	20.40
L Posteriorcingulate	1.12×10^{-04}	15.00
R Ventral diencephalon	1.21×10^{-04}	14.86
R Entorhinal	1.31×10^{-04}	14.70
R Inferiorparietal	1.36×10^{-04}	14.64
R Superiortemporal bank	1.65×10^{-04}	14.27
L Parahippocampal	2.19×10^{-04}	13.73
L Fusiform	2.45×10^{-04}	13.51
R Posteriorcingulate	3.30×10^{-04}	12.95
L Superiorparietal	3.73×10^{-04}	12.72
R Postcentral	4.82×10^{-04}	12.24

* ε indicates double floating point precision, approximately 2.22×10^{-16}

Supplementary Results and Discussion

Initial parametric tests

An initial analysis was performed to determine whether there were connectivity differences between the most face- and scene-selective voxels in the fusiform. We categorized voxels as highly face or scene selective if they responded at least two standard deviations above or below the mean, respectively, in the contrast of faces > scenes. A random effects ANOVA comparing positive and negative voxels (with participants treated as random effects) was performed per target region. Among the 85 target regions, 34 of them were significantly different between face-selective and scene-selective voxels in their fusiform connectivity, at $P < 0.05$, Bonferroni corrected (**Supplementary Table 1**). This initial finding suggested that the data possessed sufficient structure for its use in prediction. All further analyses were performed on all voxels and targets (regardless of their significance in these initial tests), treating both connectivity and functional activation as continuous variables.

Regression models excluding neighboring regions (Group 1 & 2)

As a further test of the influence of immediate spatial influence on the connectivity analysis, we included additional control models for connectivity and distance by excluding the regions neighboring the right fusiform, and compared their prediction errors. A regression model was built on Group 1 using LOOCV procedure, and tested on Group 2, as described in **Methods**. This time, however, connectivity patterns to the five regions immediately neighboring the right fusiform were excluded from the regression model. Distance models were also constructed in a similar fashion, but by training a model to predict T-values of fusiform voxels based on Euclidian distance to each target region, rather than connection probability to each target. For this analysis, distances to the neighboring cortices were also excluded from the

model. As before, the model was built from Group 1 using LOOCV, and tested on Group 2. MAE and AE were calculated as described in **Methods**, and were used to compare average and absolute prediction errors between the models with paired t-tests.

Connectivity models in the cross-validation group predicted actual fusiform activation with an MAE of 0.73 ± 0.008; this was higher than the previous model's MAE which did include connectivity to all the neighboring regions ($T(22) = 8.36$, $P = 2.81\times10^{-8}$). However, as was true for the original connectivity model, MAE comparisons between these control connectivity models and corresponding distance models (also built by excluding the neighbors) revealed better performance by connectivity ($T(22) = -3.73$, $P = 1.17\times10^{-3}$). The group-average model, which was identical to the model described in **Methods**, since it was constructed from whole-brain contrast maps using typical analysis methods, did not perform any better than the new connectivity models ($T(22) = 1.58$, $P = 0.13$).

We applied the connectivity model (excluding the neighbors) derived from all the subjects from Group 1, to the connectivity data of subjects in Group 2. While the MAEs of this new model (0.75 ± 0.009) were higher than those of the previous connectivity model ($T(20) = 4.37$, $P = 2.97\times10^{-4}$), they still outperformed the corresponding distance models by MAE ($T(20) = -8.17$, $P = 8.43\times10^{-8}$). Further, these MAEs were better than the previous group-average model, although this did not reach significance (group MAE = 0.82 ± 0.039; $T(20) = -2.01$, $P = 0.06$).

Regression models on the left fusiform gyrus

We replicated our main analyses for models of connectivity, distance, and group-average, in exactly the same manner but on the left fusiform gyrus. Comparisons of prediction errors between right and left fusiform models were performed by two-tailed t-tests (due to an unequal number of voxels in native-space left & right fusiform) while comparisons of models within the left fusiform were subject to paired t-tests as before. In Group 1, connectivity models of the left fusiform predicted the left fusiform's actual activation with an MAE of 0.67 ± 0.02; this was not worse than the prediction errors of the right fusiform models ($T(22) = 1.14$, $P = 0.27$). Just as was reported for the right fusiform, the MAE comparisons between the left fusiform's connectivity models and their corresponding distance models (MAE = 1.07 ± 0.105) revealed better performance by connectivity ($T(22) = -3.78$, $P = 1.03\times10^{-3}$). The group-average model was built identically to the procedure described in **Methods**, but the values were extracted from the left, not right fusiform. This model performed worse (MAE = 0.74 ± 0.034) than the left fusiform's connectivity model at near significance ($T(22) = 2$, $P = 0.057$).

We applied the final connectivity model for the left fusiform from Group 1 to the left fusiform connectivity data of subjects in Group 2. The MAEs of this new model (0.69 ± 0.02) were no different than those of the right fusiform connectivity model ($T(20) = 0.74$, $P = 0.47$). The left fusiform connectivity models outperformed the corresponding distance models (MAE = 0.73 ± 0.006; $T(20) = -3.09$, $P = 5.80\times10^{-3}$). Further, these MAEs were better than the corresponding group-average model (MAE = 0.82 ± 0.039; $T(20) = -3.86$, $P = 9.28\times10^{-4}$). Given previous research on the differences between the right and left fusiform's functional selectivity profiles (for faces and words respectively), a future extension of this study would be

to examine the specificity of connectivity-based models in predicting those selective responses and compare their predictive networks.